

Dual-Energy Computed Tomography Quantification of Extravasated Iodine and Hemorrhagic Transformation after Thrombectomy

Minyoul Baik,^{a,b} Jihoon Cha,^b Sung Soo Ahn,^b Seung-Koo Lee,^b Young Dae Kim,^{a,c} Hyo Suk Nam,^{a,c} Soyoung Jeon,^d Hye Sun Lee,^d Ji Hoe Heo^{a,c}

^aDepartment of Neurology, Yonsei University College of Medicine, Seoul, Korea

^bDepartment of Radiology, Yonsei University College of Medicine, Seoul, Korea

^cIntegrative Research Center for Cerebrovascular and Cardiovascular Diseases, Seoul, Korea

^dBiostatistics Collaboration Unit, Department of Research Affairs, Yonsei University College of Medicine, Seoul, Korea

Dear Sir:

After endovascular thrombectomy (EVT) for ischemic stroke, early prediction of hemorrhagic transformation (HT) is important because HT often requires changes in therapeutic strategy.¹ Parenchymal hyperdense lesions, commonly observed on brain computed tomography scans after EVT, are caused by ischemic disruption of the blood-brain barrier and may be seen with secondary contrast staining or hemorrhage.²⁻⁴ Dual-energy computed tomography (DECT) can accurately differentiate hemorrhage from contrast staining, and parenchymal contrast staining has been associated with the development of future HT.²⁻⁴ However, whether the predictability may be improved when both imaging and clinical markers are simultaneously considered and the imaging marker associated with HT volume remain unclear.

Hence, we aimed to identify quantified markers for iodine extravasation on early DECT for the occurrence and volume of HT and investigate whether the simultaneous consideration of clinical markers could improve predictability.

This single-center retrospective study included patients with acute ischemic stroke with large artery occlusion of the anterior circulation, who underwent EVT and DECT within 60 minutes after EVT between May 2019 and October 2020 (Supplementary Figure 1). The details of the study design and imaging analysis are described in the Supplementary methods and Supplementary results.³⁻¹⁸ Briefly, the volume of interest (VOI) was manually drawn by two independent readers. The VOIs covered

all areas of increased iodine concentration within the corresponding infarct territory on the iodine map of DECT. Iodine concentrations were then extracted from the VOIs of all images, and quantitative parameters were calculated (Figure 1). We determined the maximum iodine concentration and iodine extravasation volume that best predicted the occurrence and volume of HT, respectively (Supplementary Tables 1 and 2). HT was diagnosed and measured for volume with T2*-weighted gradient echo (GRE) sequences 24 hours after EVT.

Of the 56 included patients, 28 (50.0%) had HT and nine (16.1%) had parenchymal hemorrhage (Supplementary Table 3). The mean HT volume on GRE was 6.3 mL (range, 0.0 to 89.6). After adjustment for clinical variables (Supplementary Table 4), the maximum iodine concentration, defined as the iodine concentration at the 95th percentile, was the best predictor of HT occurrence (odds ratio, 8.29; 95% confidence interval, 2.30 to 29.93) (Table 1). Adding the clinical model, consisting of serum glucose level and collateral scores (Supplementary Table 4), to the maximum iodine concentration improved the prediction of HT occurrence, as measured using the area under the receiver operating curve (0.834 to 0.931, $P=0.044$) (Supplementary Figure 2). The iodine extravasation volume, defined as the volume of iodine concentration >0.7 mg/mL, showed the best correlation with HT volume ($\beta=0.44$, $R^2=0.791$, $P<0.001$, Table 1; Pearson's partial correlation coefficient $r=0.823$, $P<0.001$, Supplementary Figure 3).

Herein, the maximum iodine concentration on DECT immediately after EVT was associated with HT occurrence. This find-

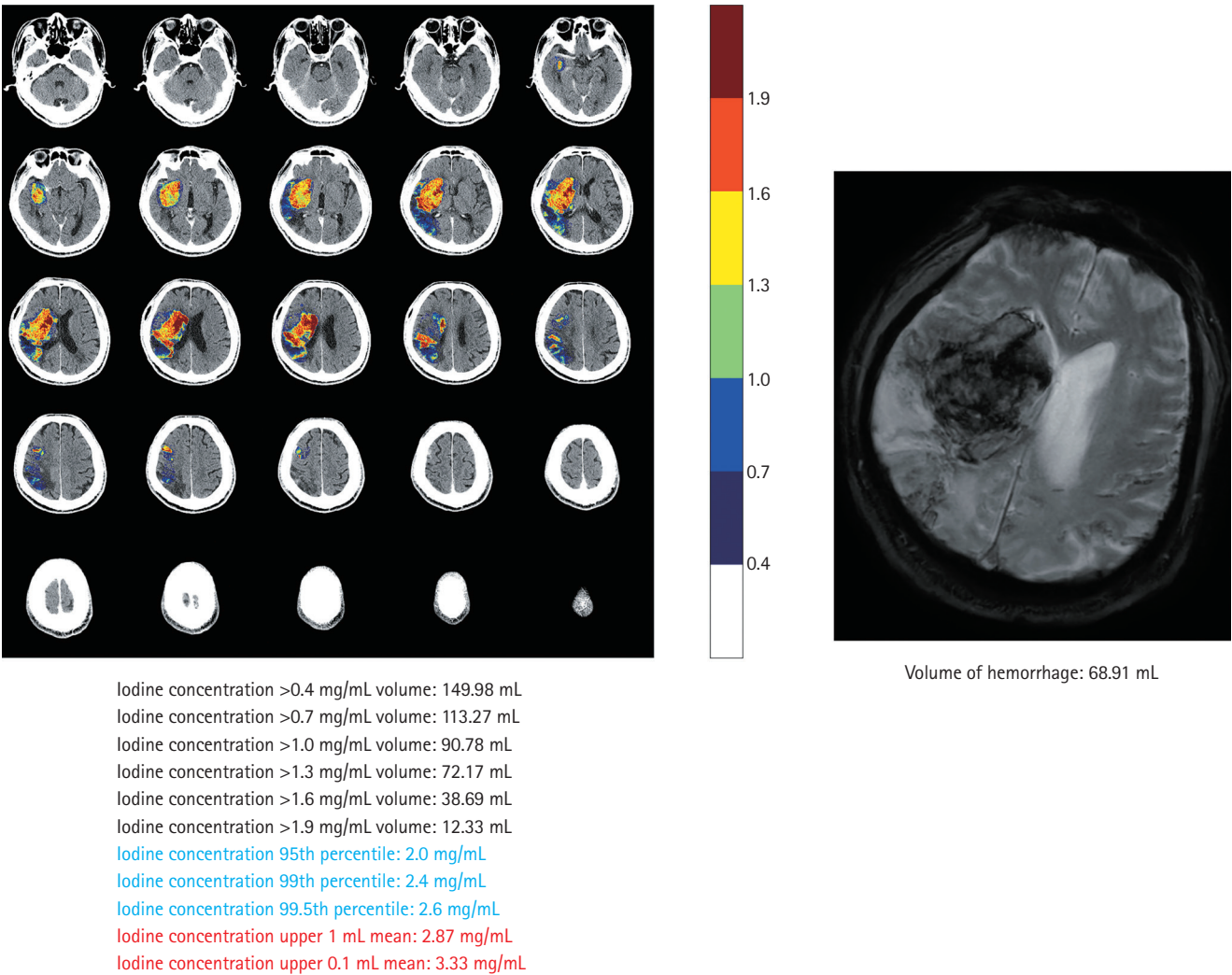


Figure 1. Iodine extravasation markers on dual-energy computed tomography and comparison with gradient echo imaging.

Table 1. Multivariable regression analysis of the iodine extravasation markers

	Occurrence of HT*		Volume of HT†		
	OR (95% CI)	P	β (SE)	R ²	P
Maximum iodine concentration‡	8.29 (2.30–29.93)	0.001	3.87 (2.03)	0.394	0.063
Volume of iodine extravasation§	1.08 (0.98–1.18)	0.120	0.44 (0.04)	0.791	<0.001

HT, hemorrhagic transformation; OR, odds ratio; CI, confidence interval; SE, standard error.

*Multivariable logistic regression with adjustment for variables with $P < 0.05$ on the univariable analyses: serum glucose level and collateral scores; †Multivariable linear regression with adjustment for variables with $P < 0.05$ on the univariable analyses: diabetes, prothrombin time, National Institutes of Health Stroke Scale, and Alberta Stroke Program Early CT Score (ASPECTS); ‡Maximum iodine concentration was defined as an iodine concentration at the 95th percentile; §Volume of iodine extravasation was defined as the voxel volume with an iodine concentration >0.7 mg/mL.

ing is consistent with those of previous studies, where the maximum iodine concentration was determined in the manually defined hotspot ROI in the selected area.^{3,4} Using a VOI-based histogram approach, we could further reduce the potential risks of selection bias and determine the better imaging

marker of iodine extravasation.¹⁹ The clinical outcomes after an EVT may be directly associated with the HT volume or parenchymal hemorrhage rather than the presence of HT itself.²⁰ We found an independent linear correlation between the iodine extravasation volume on DECT and HT on GRE. Moreover, the

prediction of HT improved when clinical variables were considered along with the imaging findings. Thus, it is necessary to consider both clinical factors and imaging markers when predicting HT. This study had some limitations. The sample size is small and most of the HTs in our study population had a small volume, which might limit its clinical impact.

In conclusion, the quantitative assessment of iodine extravasation on DECT immediately after EVT could help identify patients with a higher risk of HT development and a larger HT volume. Additionally, it would be beneficial to consider both clinical factors and imaging markers to predict HT.

Supplementary materials

Supplementary materials related to this article can be found online at <https://doi.org/10.5853/jos.2021.03391>.

References

- Jadhav AP, Molyneaux BJ, Hill MD, Jovin TG. Care of the post-thrombectomy patient. *Stroke* 2018;49:2801-2807.
- Renú A, Amaro S, Laredo C, Román LS, Llull L, Lopez A, et al. Relevance of blood-brain barrier disruption after endovascular treatment of ischemic stroke: dual-energy computed tomographic study. *Stroke* 2015;46:673-679.
- Bonatti M, Lombardo F, Zamboni GA, Vittadello F, Currò Dossi R, Bonetti B, et al. Iodine extravasation quantification on dual-energy CT of the brain performed after mechanical thrombectomy for acute ischemic stroke can predict hemorrhagic complications. *AJNR Am J Neuroradiol* 2018;39:441-447.
- Byrne D, Walsh JP, Schmiedeskamp H, Settecase F, Heran MKS, Niu B, et al. Prediction of hemorrhage after successful recanalization in patients with acute ischemic stroke: improved risk stratification using dual-energy CT parenchymal iodine concentration ratio relative to the superior sagittal sinus. *AJNR Am J Neuroradiol* 2020;41:64-70.
- Powers WJ, Rabinstein AA, Ackerson T, Adeoye OM, Bambakidis NC, Becker K, et al. Guidelines for the early management of patients with acute ischemic stroke: 2019 update to the 2018 guidelines for the early management of acute ischemic stroke: a guideline for healthcare professionals from the American Heart Association/American Stroke Association. *Stroke* 2019;50:e344-e418.
- Nogueira RG, Jadhav AP, Haussen DC, Bonafe A, Budzik RF, Bhuva P, et al. Thrombectomy 6 to 24 hours after stroke with a mismatch between deficit and infarct. *N Engl J Med* 2018;378:11-21.
- Albers GW, Marks MP, Kemp S, Christensen S, Tsai JP, Ortega-Gutierrez S, et al. Thrombectomy for stroke at 6 to 16 hours with selection by perfusion imaging. *N Engl J Med* 2018;378:708-718.
- Pasternak JJ, Williamson EE. Clinical pharmacology, uses, and adverse reactions of iodinated contrast agents: a primer for the non-radiologist. *Mayo Clin Proc* 2012;87:390-402.
- Almqvist H, Holmin S, Mazya MV. Dual energy CT after stroke thrombectomy alters assessment of hemorrhagic complications. *Neurology* 2019;93:e1068-e1075.
- Fedorov A, Beichel R, Kalpathy-Cramer J, Finet J, Fillion-Robin JC, Pujol S, et al. 3D slicer as an image computing platform for the Quantitative Imaging Network. *Magn Reson Imaging* 2012;30:1323-1341.
- Lee BI, Nam HS, Heo JH, Kim DI; Yonsei Stroke Team. Yonsei Stroke Registry. Analysis of 1,000 patients with acute cerebral infarctions. *Cerebrovasc Dis* 2001;12:145-151.
- Adams HP Jr, Bendixen BH, Kappelle LJ, Biller J, Love BB, Gordon DL, et al. Classification of subtype of acute ischemic stroke. Definitions for use in a multicenter clinical trial. TOAST. Trial of Org 10172 in Acute Stroke Treatment. *Stroke* 1993;24:35-41.
- Tan IY, Demchuk AM, Hopyan J, Zhang L, Gladstone D, Wong K, et al. CT angiography clot burden score and collateral score: correlation with clinical and radiologic outcomes in acute middle cerebral artery infarct. *AJNR Am J Neuroradiol* 2009;30:525-531.
- Barber PA, Demchuk AM, Zhang J, Buchan AM. Validity and reliability of a quantitative computed tomography score in predicting outcome of hyperacute stroke before thrombolytic therapy. ASPECTS Study Group. Alberta Stroke Programme Early CT Score. *Lancet* 2000;355:1670-1674.
- Trouillas P, von Kummer R. Classification and pathogenesis of cerebral hemorrhages after thrombolysis in ischemic stroke. *Stroke* 2006;37:556-561.
- DeLong ER, DeLong DM, Clarke-Pearson DL. Comparing the areas under two or more correlated receiver operating characteristic curves: a nonparametric approach. *Biometrics* 1988;44:837-845.
- Pencina MJ, D'Agostino RB Sr, D'Agostino RB Jr, Vasan RS. Evaluating the added predictive ability of a new marker: from area under the ROC curve to reclassification and beyond. *Stat Med* 2008;27:157-172.
- Xu C, Zhou Y, Zhang R, Chen Z, Zhong W, Gong X, et al. Metallic hyperdensity sign on noncontrast CT immediately after mechanical thrombectomy predicts parenchymal hemorrhage in patients with acute large-artery occlusion. *AJNR Am J Neuroradiol* 2019;40:661-667.

19. Law M, Young R, Babb J, Pollack E, Johnson G. Histogram analysis versus region of interest analysis of dynamic susceptibility contrast perfusion MR imaging data in the grading of cerebral gliomas. *AJNR Am J Neuroradiol* 2007;28:761-766.
20. Nogueira RG, Gupta R, Jovin TG, Levy EI, Liebeskind DS, Zaidat OO, et al. Predictors and clinical relevance of hemorrhagic transformation after endovascular therapy for anterior circulation large vessel occlusion strokes: a multicenter retrospective analysis of 1122 patients. *J Neurointerv Surg* 2015;7:16-21.

Correspondence: Jihoon Cha

Department of Radiology, Yonsei University College of Medicine, 50-1 Yonsei-ro, Seodaemun-gu, Seoul 03722, Korea

Tel: +82-2-2228-2364

Fax: +82-2-2227-8337

E-mail: JIHOONCHA@yuhs.ac

<https://orcid.org/0000-0002-1662-8041>

Received: September 27, 2021

Revised: November 8, 2021

Accepted: December 23, 2021

The authors have no financial conflicts of interest.

Supplementary methods

Study design

This study was approved by the local Institutional Review Board of Severance Hospital, Yonsei University Health System (IRB number: 4-2021-0268) with a waiver of informed consent due to the retrospective nature of this study.

First, we determined which iodine markers, including maximum iodine concentration and volume of iodine concentration, better predicted hemorrhagic transformation (HT) occurrence and volume (Supplementary Tables 1 and 2). We performed multivariable regression analysis with these iodine markers, adjusting for clinical variables, to determine correlations with HT occurrence and volume. We further investigated whether the addition of clinical variables to iodine markers could improve HT prediction.

Recanalization treatment

All patients underwent non-contrast computed tomography (CT), CT angiography, and CT perfusion (Revolution EVO, GE Healthcare, Milwaukee, WI, USA) at the emergency department on arrival. Patients were treated with intravenous alteplase (0.9 mg/kg) and/or endovascular thrombectomy (EVT) primarily based on current guidelines and recent trials.⁵⁻⁷ Omnipaque (iohexol, GE Healthcare) and Visipaque (iodixanol, GE Healthcare) were used for CT angiography and catheter angiography, respectively. The devices for EVT included the following stent retrievers: Solitaire AB/FR (ev3, Irvine, CA, USA), Trevo Proview (Stryker, Fremont, CA, USA), Embotrap II (Neuravi, Galway, Ireland), and Aperio (Acandis, Pforzheim, Germany); and aspiration catheters, Penumbra ACE (Penumbra, Alameda, CA, USA), AXS Catalyst 6 (Stryker), and Sofia (Microvention, Tustin, CA, USA). Intra-arterial tirofiban, a glycoprotein IIb/IIIa antagonist, was used as an adjuvant therapy in cases of re-occlusion. Dual-energy computed tomography (DECT) was performed immediately after the EVT. Brain magnetic resonance imaging and magnetic resonance angiography were performed 24 hours after EVT.

DECT and protocols

The patients underwent DECT (SOMATOM Force, Siemens Healthineers, Erlangen, Germany) immediately after EVT. To minimize the time factor that affects the quantification of iodine markers,^{8,9} we included only patients with DECT within 60 minutes after EVT in accordance with previous studies.^{3,4} Non-contrast CT was performed in a dual-energy acquisition with two X-ray tubes operated at 80 kV and Sn150 kV, where "Sn" denotes the use of an additional tin filter that increases

the mean photon energy of the respective spectrum. Scan parameters were as follows: collimation width, 192×0.6 mm; rotation time, 1.0 second; pitch, 0.7. The effective mA values were set to 450 mA at 80 kV and 300 mA at Sn150 kV. The volume CT dose index were 44.76 mGy.

During the study period, DECT data were unavailable at midnight. In addition, since the coronavirus disease 2019 (COVID-19) outbreak, patients with a body temperature of $\geq 37.3^{\circ}\text{C}$, or those with any symptoms associated with COVID-19, were not allowed to move from the angiographic suite or emergency department to other areas, including the CT room for DECT, until the result of reverse transcription polymerase chain reaction test for COVID-19 was reported. As such, DECT could not be performed within 60 minutes in several patients.

Image analysis of DECT

For each patient, simulated 120-kV images, virtual non-contrast images, and iodine map images were generated using a commercially available software (syngo.via, Dual-Energy CT Brain Hemorrhage application, version VA30A, Siemens Healthineers). For quantitative image analysis, the volume of interest (VOI) was manually drawn and placed in all areas with increased concentrations on the iodine map corresponding to the infarction area. The analysis was performed using a 3D slicer (<https://www.slicer.org>) by two independent readers (M.B. and J.C.).¹⁰ If there was no visible area with increased iodine concentration, the ipsilateral basal ganglia were selected as the VOI. The iodine concentration within the VOIs of all the images was extracted. Quantitative parameters were calculated as follows using python 3.7 (Python Software Foundation, <https://www.python.org/>): volumes of iodine concentration with >0.4 , >0.7 , >1.0 , >1.3 , >1.6 , and >1.9 mg/mL; iodine concentrations of 95th, 99th, and 99.5th percentile VOIs; and mean iodine concentration of 0.1 and 1 mL with the highest iodine concentration (Figure 1). The maximum iodine concentration, volume of iodine extravasation, and volume of HT showed excellent reliability between the two readers (intraclass correlation coefficients of 0.92, 0.97, and 0.93, respectively; all >0.90). The mean values recorded by the two readers were used for the statistical analysis.

Clinical and imaging data

Clinical and laboratory data were obtained from the Yonsei Stroke Registry.¹¹ Stroke subtypes, based on the Trial of ORG 10172 in the Acute Stroke Treatment classification,¹² were determined at the weekly stroke conference with a consensus among stroke neurologists. The subtypes were entered into the

registry.¹¹ The Alberta Stroke Program Early CT Score (ASPECTS) and collateral scores proposed by Tan et al.¹³ were assessed on initial non-contrast CT and CT angiography.¹⁴ HT was determined by the presence of any dark signal on gradient echo (GRE) images (conventional GRE sequence with 5 mm thickness) in the parenchyma of the corresponding infarction territory on diffusion-weighted imaging. To determine HT volume, VOIs were placed in all areas with a dark signal on the GRE image in the corresponding infarction territory. Parenchymal hemorrhage was defined in accordance with the European Cooperative Acute Stroke Study II framework.¹⁵

Statistical analyses

Statistical analyses were performed using R version 4.0.3 (<http://www.R-project.org>). Univariable analyses were performed using an independent t-test or Mann-Whitney U test for continuous variables and a chi-square test for categorical variables, as appropriate. Multivariable analysis was conducted while adjusting for significant variables ($P < 0.05$) in the univariable analyses (Supplementary Table 4). The area under curves (AUCs) were compared to find which iodine marker best predicted the HT occurrence.¹⁶ Determinants for HT occurrence were studied using univariable logistic regression analyses. AUCs were calculated to determine whether the addition of the clinical variables to DECT variables could improve HT prediction.¹⁷ We examined the correlation between the iodine

markers and the HT volume using correlation coefficients and compared them using the Steigers Z-test. We calculated the univariable linear regression β coefficients, standard errors, R^2 , and P -values to identify variables related to HT volume. Multivariable linear regression analysis was used to determine the independent correlates of the HT volume. To assess the association between HT volume and iodine markers, Pearson's partial correlation analyses were performed between HT volume and maximum iodine concentration or the volume of iodine extravasation. Statistical significance was set at $P < 0.05$.

Supplementary results

Conventional method and VOI-based histogram method

We compared the predictability of the occurrence of HT between the VOI-based histogram method (maximum iodine concentration on DECT) and the conventional method (metallic hyperdensity sign on non-contrast brain CT).¹⁶ The metallic hyperdensity sign was defined as a non-petechial intracerebral hyperdense lesion (diameter, ≥ 1 cm) in the basal ganglia and a maximum density of >90 hounsfield unit (HU) on simulated 120-kV images of DECT.¹⁸ Maximum iodine concentration better predicted the occurrence of future HT than the conventional metallic hyperdensity sign (AUCs 0.834 vs. 0.732, $P = 0.044$).

Supplementary Table 1. AUC comparison for occurrence of hemorrhagic transformation

Variable	AUC (95% CI)	P
Maximum iodine concentration		
Iodine concentration of 95%	0.834 (0.726–0.943)	Ref
Iodine concentration of 99%	0.809 (0.693–0.925)	0.181
Iodine concentration of 99.5%	0.791 (0.668–0.914)	0.109
Mean iodine concentration of upper 1 mL	0.817 (0.702–0.931)	0.501
Mean iodine concentration of upper 0.1 mL	0.796 (0.675–0.917)	0.204
Volume of iodine extravasation		
Volume of iodine concentration >0.4 mg/mL	0.751 (0.621–0.882)	0.130
Volume of iodine concentration >0.7 mg/mL	0.800 (0.683–0.918)	0.376
Volume of iodine concentration >1.0 mg/mL	0.809 (0.696–0.922)	0.403
Volume of iodine concentration >1.3 mg/mL	0.783 (0.656–0.909)	0.161
Volume of iodine concentration >1.6 mg/mL	0.795 (0.672–0.917)	0.283
Volume of iodine concentration >1.9 mg/mL	0.804 (0.689–0.919)	0.401

The maximum iodine concentration was defined as the iodine concentration at the 95th percentile because the AUC (0.834; 95% CI, 0.726 to 0.943) tended to be higher than that of other iodine concentrations. A cut-off value of 1.70 mg/mL allowed us to identify patients who developed hemorrhagic transformation with 67.9% sensitivity and 89.3% specificity.

AUC, area under curve; CI, confidence interval.

Supplementary Table 2. Correlation coefficient comparison for volume of hemorrhagic transformation

Variable	R (95% CI)	P
Maximum iodine concentration		
Iodine concentration of 95%	0.391 (0.142–0.593)	<0.001
Iodine concentration of 99%	0.376 (0.125–0.581)	<0.001
Iodine concentration of 99.5%	0.403 (0.157–0.602)	<0.001
Mean iodine concentration of upper 1 mL	0.577 (0.370–0.729)	<0.001
Mean iodine concentration of upper 0.1 mL	0.569 (0.360–0.724)	<0.001
Volume of iodine extravasation		
Volume of iodine concentration >0.4 mg/mL	0.830 (0.726–0.897)	0.136
Volume of iodine concentration >0.7 mg/mL	0.845 (0.749–0.907)	Ref
Volume of iodine concentration >1.0 mg/mL	0.819 (0.709–0.890)	0.013
Volume of iodine concentration >1.3 mg/mL	0.774 (0.642–0.862)	<0.001
Volume of iodine concentration >1.6 mg/mL	0.699 (0.534–0.812)	<0.001
Volume of iodine concentration >1.9 mg/mL	0.597 (0.397–0.743)	<0.001

The correlation coefficient between the volume of iodine concentration >0.7 mg/mL and the hemorrhagic transformation volume was higher than that of other iodine volume parameters. Hence, voxels with an iodine concentration >0.7 mg/mL were used to determine the volume of iodine extravasation.

CI, confidence interval.

Supplementary Table 3. Demographic characteristics of patients stratified by hemorrhagic transformation

Characteristic	Hemorrhagic transformation		P
	Yes (n=28)	No (n = 28)	
Medical history			
Age (yr)	72.0±14.8	69.6±13.0	0.530
Male sex	20 (71.4)	15 (53.6)	0.270
Hypertension	21 (75.0)	21 (75.0)	>0.999
Diabetes mellitus	15 (53.6)	9 (32.1)	0.177
Dyslipidemia	8 (28.6)	11 (39.3)	0.572
Old stroke	6 (21.4)	7 (25.0)	>0.999
Ischemic heart disease	6 (21.4)	3 (10.7)	0.467
Peripheral artery occlusive disease	2 (7.1)	3 (10.7)	>0.999
Current smoker	7 (25.0)	5 (17.9)	0.745
Atrial fibrillation	15 (53.6)	15 (53.6)	>0.999
Prior antithrombotics use	16 (57.1)	10 (35.7)	0.180
Antiplatelet agents	12 (42.9)	5 (17.9)	0.081
Anticoagulants	7 (25.0)	6 (21.4)	>0.999
Pre-mRS	0.0 (0.0–0.0)	0.0 (0.0–0.5)	0.756
Pre-mRS ≤2	27 (96.4)	26 (92.9)	>0.999
Initial SBP (mm Hg)	159.1±30.0	148.9±27.5	0.187
Laboratory findings			
Platelet counts (×10 ⁹ /L)	230.2±72.6	236.0±81.4	0.777
PT, INR	1.0 (1.0–1.1)	1.0 (1.0–1.1)	>0.999
aPTT (sec)	29.1 (27.5–32.5)	29.0 (27.1–31.9)	0.676
Serum glucose (mmol/L)	8.3 (6.4–11.0)	6.5 (5.7–7.6)	0.009
eGFR (mL/min/1.73 m ²)	75.6±21.6	81.9±17.0	0.237
Stroke characteristics			
Initial NIHSS	12.0±6.4	11.9±7.4	0.954
ASPECTS	7.5 (6.0–9.0)	9.0 (8.0–9.0)	0.071
ASPECTS ≥6	25 (89.3)	26 (92.9)	>0.999
Collateral scores	1.0 (1.0–2.0)	2.0 (1.5–2.0)	0.003
Collateral score ≥2	11 (39.3)	21 (75.0)	0.015
TOAST CE (vs. non-CE)	18 (64.3)	13 (46.4)	0.282
TOAST			0.175
CE	18 (64.3)	13 (46.4)	
LAA	6 (21.4)	6 (21.4)	
Other determined	2 (7.1)	1 (3.6)	
Undetermined	2 (7.1)	3 (10.7)	
More than two causes	0 (0)	5 (17.9)	
IV-tPA	12 (42.9)	10 (35.7)	0.784
IA-tirofiban	4 (14.3)	4 (14.3)	>0.999
No. of stent retriever passes	1.0 (1.0–2.0)	1.0 (1.0–2.0)	0.796
Onset to puncture (min)	335.0 (190.5–717.0)	304.5 (201.5–596.5)	0.954
TICI grade 3	16 (57.1)	18 (64.3)	0.784
Imaging characteristics			
Closing to DECT (min)	24.0 (19.5–34.0)	25.0 (19.5–29.5)	0.737
Closing to MRI (hr)	13.5 (11.0–16.0)	14.0 (12.0–18.0)	0.444
Outcome variables			
mRS at discharge	4.5 (2.0–5.0)	2.5 (1.0–5.0)	0.083
mRS at discharge ≤2	9 (32.1)	14 (50.0)	0.277
mRS at 3 months (n=52)	3.0 (1.0–6.0)	2.0 (0.5–4.0)	0.257
mRS at 3 months ≤2 (n=52)	12 (48.0)	14 (51.9)	>0.999

Values are presented as mean±standard deviation, number (%), or median (interquartile range).

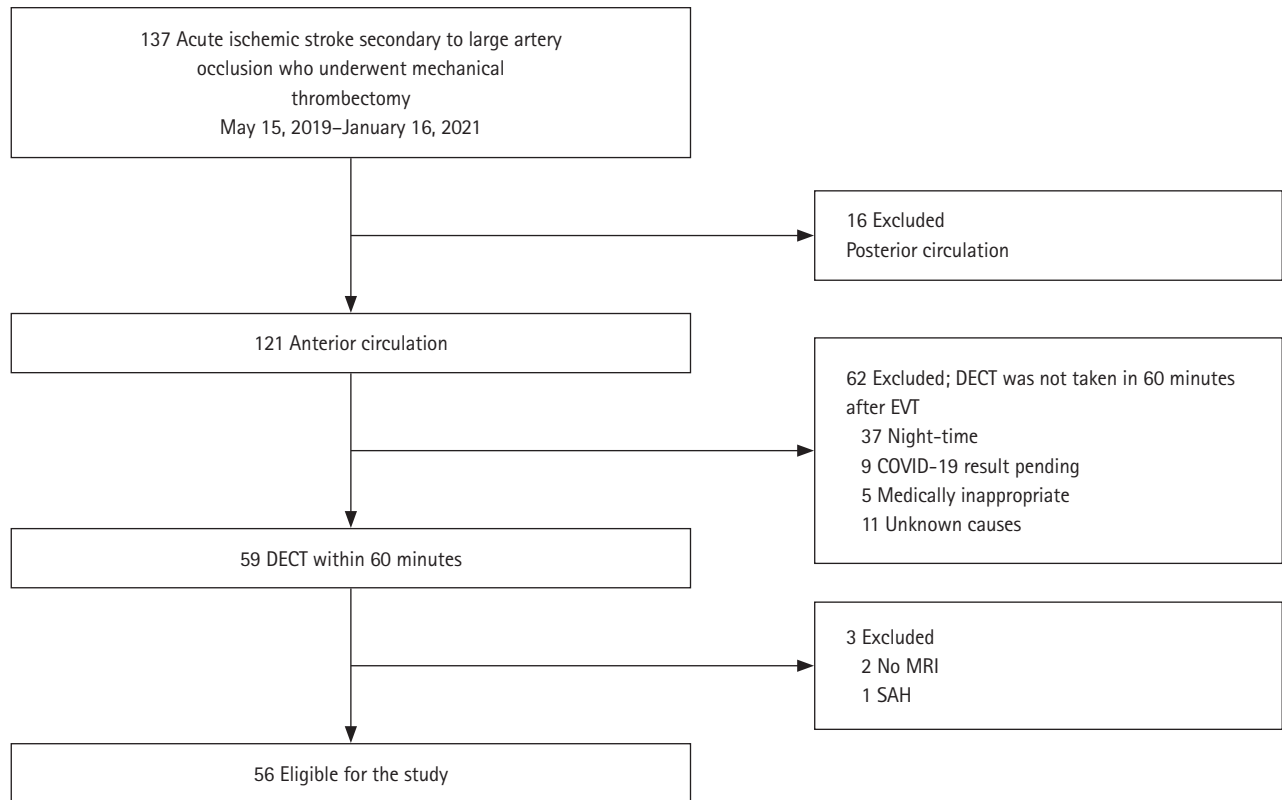
mRS, modified Rankin Scale; SBP, systolic blood pressure; PT, prothrombin time; INR, international normalized ratio; aPTT, activated partial thromboplastin time; eGFR, estimated glomerular filtration rate; NIHSS, National Institutes of Health Stroke Scale; ASPECTS, Alberta Stroke Program Early CT Score; TOAST, Trial of ORG 10172 in Acute Stroke Treatment; CE, cardioembolism; LAA, large artery atherosclerosis; IV, intravenous; tPA, tissue plasminogen activator; IA, intra-arterial; TICI, thrombolysis in cerebral infarction; DECT, dual-energy computed tomography; MRI, magnetic resonance imaging.

Supplementary Table 4. Univariable regression analysis

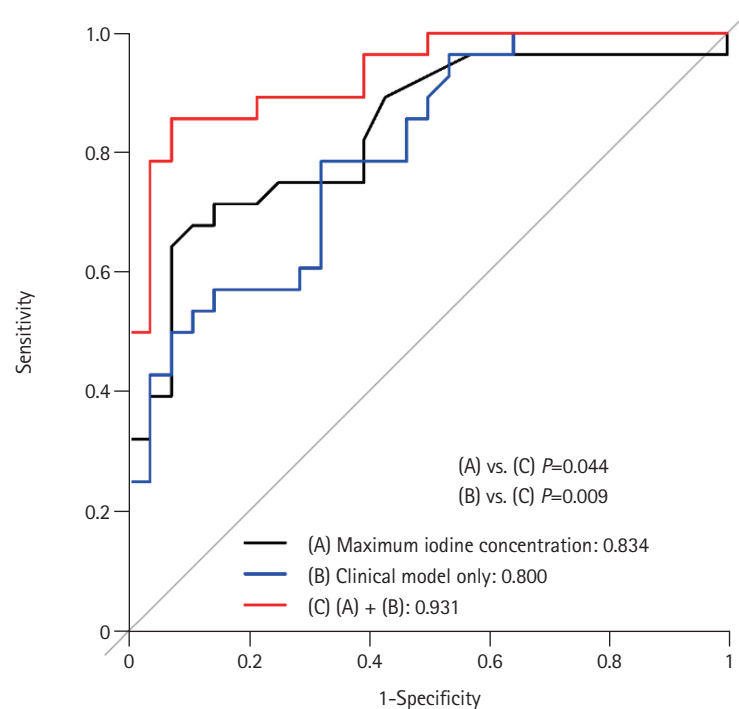
Variable	Occurrence of hemorrhagic transformation		Volume of hemorrhagic transformation	
	OR (95% CI)	P	β (SE)	P
Medical history				
Age (yr)	1.01 (0.97–1.05)	0.523	0.05 (0.17)	0.755
Male sex	2.17 (0.73–6.77)	0.171	−0.48 (4.92)	0.923
Hypertension	1.00 (0.29–3.41)	>0.999	7.31 (5.42)	0.183
Diabetes mellitus	2.44 (0.84–7.45)	0.108	11.57 (4.55)	0.014
Dyslipidemia	0.62 (0.20–1.88)	0.399	−6.43 (4.96)	0.200
Old stroke	0.82 (0.23–2.86)	0.752	5.48 (5.60)	0.332
Ischemic heart disease	2.27 (0.53–11.79)	0.283	6.39 (6.43)	0.325
Peripheral artery occlusive disease	0.64 (0.08–4.18)	0.641	7.30 (8.30)	0.383
Current smoker	1.53 (0.42–5.89)	0.516	−6.26 (5.75)	0.281
Atrial fibrillation	1.00 (0.35–2.88)	>0.999	2.37 (4.77)	0.622
Prior antithrombotics use	2.40 (0.83–7.24)	0.111	4.41 (4.74)	0.357
Initial SBP (mm Hg)	1.01 (0.99–1.03)	0.187	0.10 (0.08)	0.246
Laboratory findings				
Platelet counts ($\times 10^9/L$)	1.00 (0.99–1.00)	0.773	−0.02 (0.03)	0.630
PT, INR	3.14 (0.93–130.42)	0.307	3.55 (1.73)	0.044
aPTT (sec)	1.06 (0.94–1.22)	0.333	−0.13 (0.54)	0.814
Serum glucose (mmol/L)	1.40 (1.09–1.94)	0.023	0.96 (0.61)	0.118
eGFR (mL/min/1.73 m ²)	0.98 (0.95–1.01)	0.236	−0.16 (0.12)	0.189
Stroke characteristics				
Initial NIHSS	1.00 (0.93–1.08)	0.953	0.69 (0.34)	0.044
ASPECTS	0.73 (0.51–1.01)	0.070	−5.02 (1.16)	<0.001
ASPECTS ≥ 6	0.64 (0.08–4.18)	0.641		
Collateral scores	0.22 (0.07–0.58)	0.004	−7.13 (3.74)	0.062
Collateral score ≥ 2	0.22 (0.07–0.65)	0.009		
TOAST CE (vs. non-CE)	2.08 (0.72–6.22)	0.181	6.93 (4.70)	0.147
IV-tPA	1.35 (0.46–4.02)	0.585	−6.78 (4.79)	0.163
IA-tirofiban	1.00 (0.21–4.68)	>0.999	−0.65 (6.81)	0.924
No. of stent retriever passes	0.86 (0.49–1.48)	0.588	−0.82 (2.43)	0.737
Onset to puncture (min)	1.00 (1.00–1.00)	0.546	0.00 (0.00)	0.623
TICI grade 3	0.74 (0.25–2.17)	0.585	2.10 (4.87)	0.669
Imaging characteristics				
Closing to DECT (min)	1.01 (0.96–1.06)	0.699	0.24 (0.22)	0.283
Closing to MRI (hr)	0.97 (0.91–1.02)	0.287	−0.16 (0.21)	0.461
Iodine markers				
Maximum iodine concentration	6.21 (2.28–16.92)	< 0.001	6.45 (2.07)	0.003
Volume of iodine extravasation	1.09 (1.00–1.18)	0.050	0.48 (0.04)	<0.001

Among the clinical variables, the serum glucose level at admission and collateral scores were associated with the occurrence of hemorrhagic transformation (HT) in univariable logistic regression analyses. The maximum iodine concentration was associated with HT occurrence, whereas the volume of iodine extravasation was not. In the univariable linear regression analyses, HT volume was associated with diabetes, prothrombin time, NIHSS score, ASPECTS score, maximum iodine concentration, and volume of iodine extravasation.

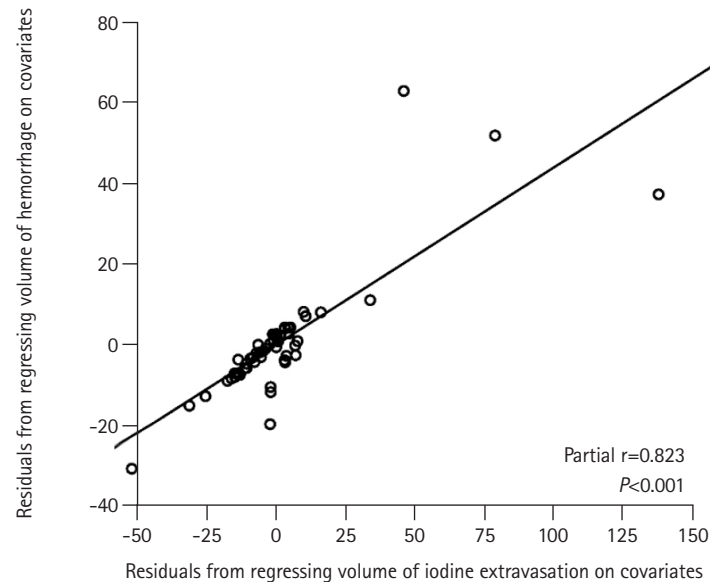
OR, odds ratio; CI, confidence interval; SE, standard error; SBP, systolic blood pressure; PT, prothrombin time; INR, international normalized ratio; aPTT, activated partial thromboplastin time; eGFR, estimated glomerular filtration rate; NIHSS, National Institutes of Health Stroke Scale; ASPECTS, Alberta Stroke Program Early CT Score; TOAST, Trial of ORG 10172 in acute stroke treatment; CE, cardioembolism; IV, intravenous; tPA, tissue plasminogen activator; IA, intra-arterial; TICI, thrombolysis in cerebral infarction; DECT, dual-energy computed tomography; MRI, magnetic resonance imaging.



Supplementary Figure 1. Patient selection. DECT, dual-energy computed tomography; EVT, endovascular thrombectomy; COVID-19, coronavirus disease 2019; MRI, magnetic resonance imaging; SAH, subarachnoid hemorrhage.



Supplementary Figure 2. Additive predictive value of maximum iodine concentration on dual-energy computed tomography after endovascular thrombectomy for ischemic stroke measured by comparison of area under curve (AUC). We evaluated whether hemorrhagic transformation (HT) prediction was improved by adding a clinical model consisting of serum glucose levels and collateral scores to the maximum iodine concentration. The AUC for HT occurrence was 0.800 (95% confidence interval [CI], 0.687 to 0.914) for the clinical model and 0.834 (95% CI, 0.726 to 0.943) for the maximum iodine concentration alone. When both the clinical model and maximum iodine concentration were considered, the AUC increased to 0.931 (95% CI, 0.867 to 0.995; $P=0.044$), with 85.7% sensitivity and 92.9% specificity.



Supplementary Figure 3. Relationship between volume of hemorrhagic transformation and volume of iodine extravasation on dual-energy computed tomography after endovascular thrombectomy for ischemic stroke measured by Pearson's partial correlation coefficient after adjusting for clinical variables. The volume of iodine extravasation showed a significant correlation with the hemorrhagic transformation (HT) volume after adjusting for clinical variables; diabetes, prothrombin time, National Institutes of Health Stroke Scale (NIHSS), Alberta Stroke Program Early CT Score (ASPECTS) (partial $r=0.823$, $P<0.001$). However, the maximum iodine concentration was not correlated (Pearson's partial correlation coefficient $r=0.260$, $P=0.063$) with the HT volume. The y-axes are based on the calculated residuals from regressing hemorrhage volume on diabetes, prothrombin time, NIHSS, and ASPECTS. The x-axes are based on the calculated residuals from the regressing volume of iodine extravasation on diabetes, prothrombin time, NIHSS, and ASPECTS. r , Pearson's partial correlation coefficient ($r=0$, no linear relationship; $r=1$ or -1 , perfect linear relationship).